

See discussions, stats, and author profiles for this publication at: <https://www.researchgate.net/publication/5278895>

Detection of Trace Hg 2+ via Induced Circular Dichroism of DNA Wrapped Around Single-Walled Carbon Nanotubes

ARTICLE in JOURNAL OF THE AMERICAN CHEMICAL SOCIETY · AUGUST 2008

Impact Factor: 12.11 · DOI: 10.1021/ja801793k · Source: PubMed

CITATIONS

71

READS

62

13 AUTHORS, INCLUDING:



Xueyun Gao

Chinese Academy of Sciences

84 PUBLICATIONS 2,923 CITATIONS

SEE PROFILE



Gengmei Xing

Chinese Academy of Sciences

68 PUBLICATIONS 2,370 CITATIONS

SEE PROFILE



Yanlian Yang

National Center for Nanoscience and Tech...

167 PUBLICATIONS 3,663 CITATIONS

SEE PROFILE



Yuliang Zhao

Chinese Academy of Sciences

345 PUBLICATIONS 11,659 CITATIONS

SEE PROFILE

Detection of Trace Hg²⁺ via Induced Circular Dichroism of DNA Wrapped Around Single-Walled Carbon Nanotubes

Xueyun Gao,^{*,#} Gengmei Xing,[#] Yanlian Yang,[†] Xiaoli Shi,[§] Ru Liu,[#] Weiguo Chu,[†] Long Jing,[#] Feng Zhao,[#] Chang Ye,[#] Hui Yuan,[#] Xiaohong Fang,[§] Chen Wang,[†] and Yuliang Zhao^{*,#}

Laboratory for Bio-Environmental Effects of Nanomaterials and Nanosafety, Institute of High Energy Physics, Beijing 100049, National Center for Nanosciences and Technology, Beijing 100080, and Key Laboratory of Molecular Nanostructure and Nanotechnology, Beijing National Laboratory for Molecular Sciences, Institute of Chemistry, Beijing 100080, Chinese Academy of Science, P. R. China

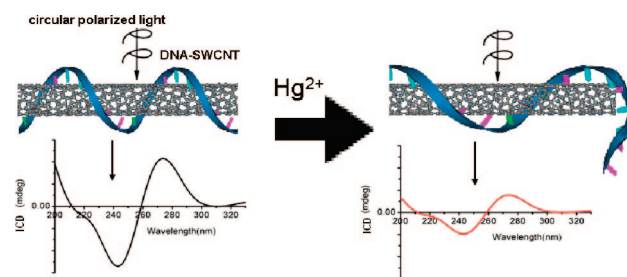
Received March 11, 2008; E-mail: gaoxy@ihep.ac.cn; zhaoyuliang@ihep.ac.cn

The conductivity and fluorescent properties of singled-wall carbon nanotubes (SWCNTs) have been well developed to detect trace molecules in solution.^{1–3} However, the chiral properties of SWCNTs have not been well studied and applied. In theory, induced circular dichroism (ICD) will occur for DNA wrapped around SWCNTs (DNA-SWCNTs) when the transition dipole moments of the optically active chiral SWCNTs couple to the transition dipole moments of DNA, thereby producing a strong ICD signal.⁴ The ICD of DNA-SWCNTs could be used to detect chemicals which can disturb the coupling effect of the transition dipole moments between DNA and SWCNTs and thus change the ICD signals significantly. Here, evidence to support this principle is disclosed.

We have found that Hg ions have a strong and specific binding affinity for the nucleic bases of single-strand DNA (T bases) wrapped around SWCNTs via a pseudo-first-order kinetic interaction. When the Hg²⁺ ions bind to the DNA bases, the tightness of the DNA wrapping around the SWCNTs is loose; in addition a repulsive electrostatic force will be introduced along the DNA strand causing the DNA to stretch. This stretching leads to a part of the DNA becoming detached from the SWCNT surface. It is expected that these disassociations will loosen the overall interaction between DNA and SWCNTs, further decreasing the coupling effects of the transition dipole moments between these two species, causing the ICD signal of DNA-SWCNTs to decrease significantly. Combining all this knowledge together, we have designed a new type of sensor to detect trace Hg ions at the nM level by monitoring the ICD of DNA-SWCNTs. In this sensor, the Hg ions interact with the bases of single-strand DNA causing the interaction between the DNA and SWCNTs to weaken, and the ICD signal to greatly decrease. The working mechanism of the DNA-SWCNT sensor is illustrated in Scheme 1.

The DNA-SWCNT sensor was fabricated via ultrasonication methods (see S1 in Supporting Information). The titration studies of the interaction between Hg ions and DNA-SWCNTs were carried out as follows: different amounts of Hg ions were introduced into the solution of DNA-SWCNTs, respectively. These samples include A1 (Hg: 0nM), A2 (Hg: 18nM), A3 (Hg: 187nM), and A4 (Hg: 1870nM), in which the concentration of DNA-SWCNTs (DNA base: 4 μM, SWCNT: 1.1 mg/L) is fixed for all samples. The sample solutions were incubated for 24 h to ensure that the reaction between the DNA bases and Hg ions is balanced via a pseudo-first-order kinetic process (see Scheme S2-1, eq 1, and eq 2 in S2 in Supporting Information).⁵ These Hg-treated DNA-SWCNTs were observed by atomic force microscopy (AFM), the microstructures of DNA-

Scheme 1. Illustrations of Hg-Induced ICD Signal Intensity Change of DNA-SWCNTs^a



^a The Hg ions binding to the DNA bases result in a DNA pitch increase and part of the DNA disassociates from the SWCNTs, leading to a significant decrease in the ICD of the DNA-SWCNTs.

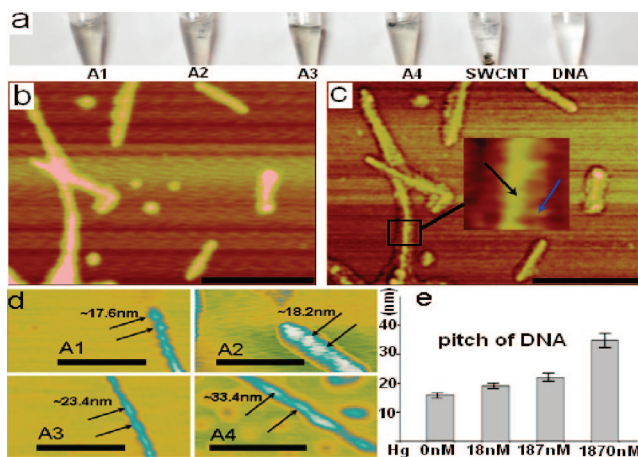


Figure 1. AFM observations of DNA-SWCNTs. (a) Optical images of DNA-SWCNTs (DNA base, ~4 μM; SWCNT, ~1.1 mg/L) at different Hg concentrations, A1 (0nM Hg), A2 (18nM), A3 (187nM), and A4 (1870nM), in which free SWCNTs and DNA are used as controls. (b) Height and (c) phase images of A1 samples; insets are the hard SWCNTs wrapped by soft DNA indicated by black and blue arrows, respectively; scale bar ≈ 200 nm. (d) Typical pitch of A1, A2, A3, A4 are indicated by arrows, scale bar ≈ 100nm. (e) The relationship between the Hg concentration and average DNA pitch of A1, A2, A3, A4 is shown by rectangular bars for each.

SWCNTs were checked to confirm whether a part of the DNA detaches from the SWCNT (see S3 in Supporting Information). Figure 1a shows that the Hg-treated DNA-SWCNT samples are very soluble and no aggregation or deposition occurred even after storage for 4 months. Figure 1b and Figure 1c reveal the typical AFM images of Hg-free DNA-SWCNTs (A1 sample), wherein the

[#] Institute of High Energy Physics.

[†] National Center for Nanosciences and Technology.

[§] Institute of Chemistry.

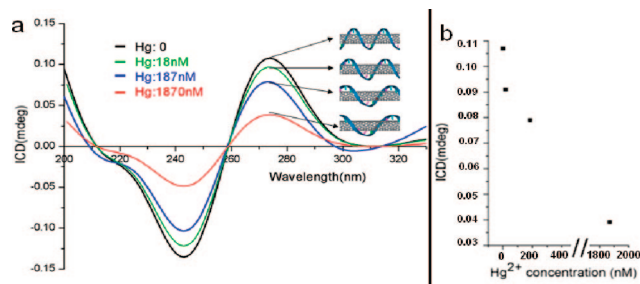


Figure 2. ICD spectra of DNA-SWCNTs at different Hg concentrations. (a) The ICD spectra of DNA-SWCNTs (DNA base $\approx 4 \mu\text{M}$, SWCNT $\approx 1.1 \text{ mg/L}$) at Hg of 0 (black curve), 18 (green curve), 187 (blue curve), and 1870 nM (red curve). Insets are illustrations of DNA-SWCNTs, where the DNA pitch is the reverse of the Hg concentration. (b) Relation between the ICD intensity of DNA-SWCNTs and Hg concentration: the ICD signal decreases as the Hg concentration increases.

DNA-SWCNTs are well dispersed on mica. The phase images in Figure 1c clearly disclose the contrast difference between the hard SWCNTs and soft DNA, where the DNA bases are tightly associated with the SWCNTs. AFM observation of A2, A3, and A4 samples are similar to that of A1 samples shown in Figure 1b and Figure 1c. However, high resolution AFM images disclosed that the pitch of DNA wrapped around SWCNT increases when the DNA-SWCNTs are exposed to different amounts of Hg in solution. Figure 1d reveals that the typical pitch of DNA wrapped around SWCNTs in the A1, A2, A3, and A4 samples are 17.6, 18.2, 23.4, and 33.4 nm, respectively. To obtain a more accurate measurement of the pitch of DNA wrapped around SWCNTs, four DNA-SWCNTs of each sample are measured, respectively. Figure 1e discloses that the DNA-SWCNTs have different pitches including 16.2 ± 1.5 (A1), 19.5 ± 2 (A2), 23.1 ± 2.4 (A3), 34 ± 3.2 nm (A4). This means that introducing Hg ions into the DNA-SWCNT solution results in the pitch of DNA increasing in a Hg-dependent manner.

To study how Hg-dependent DNA disassociation from SWCNTs (including a weakening of the DNA wrapping around the SWCNTs and a part of the DNA detaching from the SWCNTs) influences the ICD of DNA-SWCNTs, the samples (A1, A2, A3, A4) were observed using the CD spectrophotometer of the Beijing Synchrotron Radiation Facility (see S4 in Supporting Information). We observed the ICD signals between 200 and 320 nm because this spectral region contains the E44 and higher nanotube electronic transitions as well as the T and G base transitions of DNA;^{6,7} the ICD intensity of the DNA-SWCNTs will be strong because of the coupling effects of the transition dipole moment between DNA and SWCNTs. Figure 2a shows the ICD signals of the DNA-SWCNT samples in solution containing different concentrations of Hg ions, including A1 (0 nM Hg), A2 (18 nM Hg), A3 (187 nM Hg), and A4 (1870 nM Hg). All ICD spectra exhibit a positive peak at 274 nm, a negative peak at 243 nm, and a crossover point at 259 nm. The intensities of the positive peaks corresponding to A1, A2, A3, and A4 are 0.107, 0.091, 0.079, 0.039, respectively, and their negative peak intensity shows a similar Hg dependence. This revealed that Hg ions can decrease the intensity of the ICD signal in a concentration-dependent manner (shown in Figure 1d and Figure 1e, Scheme S2-2 in S2, Figure S3-1 and Figure S3-2 in S3 of Supporting Information). The relation between the ICD intensity and Hg ion concentration in solution is shown in Figure 2b, where

the ICD intensity decreases significantly while the concentration of Hg ions (A1, A2, A3, A4) increases.

Why the Hg ions interact with the DNA bases and cause the DNA to disassociate from the SWCNTs is unknown. We found that the Hg ions could strongly interact with the DNA bases (T base) of DNA-SWCNTs via a pseudo-first-order kinetic reaction, the binding constant (K_b) of Hg ions to the DNA bases is about $\sim 3.98 \times 10^6 \text{ L mol}^{-1}$ (see Scheme S2-1, eq 1, eq 2, and Figure S2-3 in S2 of Supporting Information). For DNA-SWCNTs, the Hg^{2+} -DNA base adduct will not only weaken the interaction between the DNA and SWCNTs but also introduce a repulsive, electrostatic force along the DNA strand, which will stretch the DNA strand and induce the DNA pitch to increase along the SWCNTs. In a Hg-free solution, the DNA wraps around the SWCNTs in a regular helical arrangement along the whole nanotube,⁸ but Hg-induced extending of DNA wrapped on SWCNT will cause a part of the DNA to detach from the SWCNTs (see Scheme S2-2 in S2, Figure S3-1 and Figure S3-2 in S3 of Supporting Information). Recently, numerical studies also revealed that electrostatic interactions within the ssDNA wrapped around SWCNTs will modulate the ssDNA pitch along the SWCNT axial,¹⁰ which is strong evidence to support our experimental results herein.

In summary, the ICD characteristics of DNA-SWCNTs are first used to detect trace Hg ions in solution. Our DNA-SWCNTs sensors are easy to fabricate and use in detecting mercury ions at the nM level in solution. Such DNA-SWCNT sensors may be used to detect versatile molecules if they can specifically interfere with the interaction between SWCNTs and DNA.

Acknowledgment. We are thankful for the funding supports from the NSFC (Grants 10525524, 10675141, 20571076), 973 program (Grants 2007CB935604, 2006CB705601), and the CAS Knowledge Innovation Program.

Supporting Information Available: Preparations of DNA-SWCNTs, studies of the reaction between Hg ions and DNA-SWCNTs, AFM observation of DNA-SWCNTs, CD studies of free DNA and DNA-SWCNTs, and near IR observations of DNA-SWCNTs. This materials is available free of charge via the Internet at <http://pubs.acs.org>.

References

- (1) Kim, S. N.; Rusling, J. F.; Papadimitrakopoulos, F. *Adv. Mater.* **2007**, *19*, 3214–3228.
- (2) (a) Star, A.; Tu, E.; Niemann, J.; Gabriel, J. P.; Joiner, C. S.; Valcke, C. *Proc. Natl. Acad. Sci. U.S.A.* **2006**, *103*, 921–926. (b) Katz, E.; Willner, I. *ChemPhysChem* **2004**, *5*, 1084–1104.
- (3) Satishkumar, B. C.; Brown, L. O.; Gao, Y.; Wang, C. C.; Wang, H. L.; Doorn, S. K. *Nat. Nanotechnol.* **2007**, *2*, 560–564.
- (4) Ardhamar, M.; Norden, B.; Kurucsev, T. DNA-Drug interactions. In *Circular Dichroism: Principles and Applications*, 2nd ed.; Berova, N., Nakanishi, K., Woody, R., Eds.; Wiley-VCH: New York, 2000.
- (5) (a) Li, Y.; Jiang, Y.; Yan, X. P. *Anal. Chem.* **2006**, *78*, 6115–6120. (b) Babkina, S. S.; Ulakhovich, N. A. *Bioelectrochemistry* **2004**, *63*, 261–265. (c) Scatchard, G. *Ann. N.Y. Acad. Sci.* **1949**, *51*, 660–672.
- (6) Bachilo, S. M.; Strano, M. S.; Kittrell, C.; Hauge, R. H.; Smalley, R. E.; Weisman, R. B. *Science* **2002**, *298*, 2361–2366.
- (7) Hughes, M. E.; Brandin, E.; Golovchenko, J. A. *Nano Lett.* **2007**, *7*, 1191–1194.
- (8) Gigliotti, B.; Sakizze, B.; Bethune, D. S.; Shelby, R. M.; Cha, J. N. *Nano Lett.* **2006**, *6*, 159–164.
- (9) Zheng, M.; Jagota, A.; Strano, M. S.; Santos, A. P.; Barone, P.; Chou, S. G.; Diner, B. A.; Dresselhaus, M. S.; McLean, R. S.; Onoa, G. B.; Samsonidze, G. G.; Semke, E. D.; Usrey, M.; Walls, D. J. *Science* **2003**, *302*, 1545–1548.
- (10) Johnson, Robert R.; Johnson, A. T. C.; Klein, Michael L. *Nano Lett.* **2008**, *8*, 69–75.

JA801793K